

STUDIES ON THE INFLUENCE OF ROTOR DISTANCE ON THE EFFICIENCY OF A COAXIAL ROTOR SYSTEM

Matthias Kränzler, matthias.kraenzler@de.bosch.com

Research Scientist, Corporate Research Robert-Bosch GmbH (Germany)

Sebastian Dufhaus, sebastian.dufhaus@ilr.rwth-aachen.de

Research Scientist, Institute of Aerospace Systems RWTH Aachen University (Germany)

Eike Stumpf, eike.stumpf@ilr.rwth-aachen.de

Head of Institute, Institute of Aerospace Systems RWTH Aachen University (Germany)

Abstract

Coaxial rotor systems are of special interest on aircraft with electric propulsion. An experimental analysis of the performance of such a system is described in this paper. Two rotors with identical geometry are operated at an equal rotational speed. The presented test bench allows to measure electrical and force data individually for both rotors. Analyses are conducted in the hover case as well as in a case with an axial incidence flow in a wind tunnel for various rotor separation distances. Efficiency of the rotor system is compared to a single rotor. It is shown that the separation distance of the rotors has a strong influence on the upper and lower rotor individually, although the combined performance is approximately independent in the hover case. In the case with an axial incidence flow, overall efficiency of the analyzed rotor system increases for a smaller rotor separation distance.

NOMENCLATURE

A	rotor disk area
C_T	thrust coefficient
C_P	power coefficient
D	rotor diameter
H	vertical rotor separation distance
J	advance ratio
M	torque
n	rotational speed
P_{ideal}	ideal power
P_{real}	measured power
rpm	revolutions per minute
$T_{measured}$	measured thrust
η	efficiency rotor in propeller mode
ρ	air density
v	velocity
CAN	Controller Area Network
FOM	Figure of Merit (rotor)
PIV	Particle Image Velocimetry

SUBSCRIPTS

low	lower rotor
upp	upper rotor
$isolated$	isolated rotor
$coax$	coaxial rotor
$comb$	combined

1. INTRODUCTION

The development of new battery and electric engine technologies opens up the market for electrified mobility in aviation. For example in megacities, mobility in the third dimension can relieve traffic flows. Limited landing areas and ground infrastructure in urban environments [1] postulate strict vehicle size restrictions and require future aerial vehicles to take-off and land vertically. Multi-rotor concepts are a suitable configuration for this purpose. One of the main factors for the performance and dimensions of such an aerial vehicle is the rotor system. A promising concept for a volumetric compact rotor system is the coaxial rotor configuration [2].

Classical coaxial helicopter systems are designed for a torque balanced condition in order to avoid the need for a tail rotor. The study presented in this paper focuses on the performance of a coaxial rotor system that can be used for multi-rotor systems. Such a multi-rotor aircraft is not forced to ensure torque balance for each individual coaxial rotor system, unlike it's necessary for a classical coaxial helicopter. Therefore, the two rotors can principally now be operated at different operating points. This study focuses on an operation point without torque balance performed on rotors with equal geometry and dimensions, operated at identical rotational speeds.

In this study the influence of the vertical separation distance on the efficiency of the rotor system is analysed. The investigation is independent of a specific vehicle configuration, thus it contains the hover case as well as cases of different incident

flow conditions. The upper and lower rotor system will be separately analysed to evaluate their aerodynamic performance.

2. THEORETICAL BACKGROUND

Two rotors that are operating closely together, will influence the aerodynamic conditions of each other. The wakes for a coaxial rotor system are schematically illustrated in Figure 1. The wake of the upper rotor is contracting and hits the lower rotor disk at the interference area.

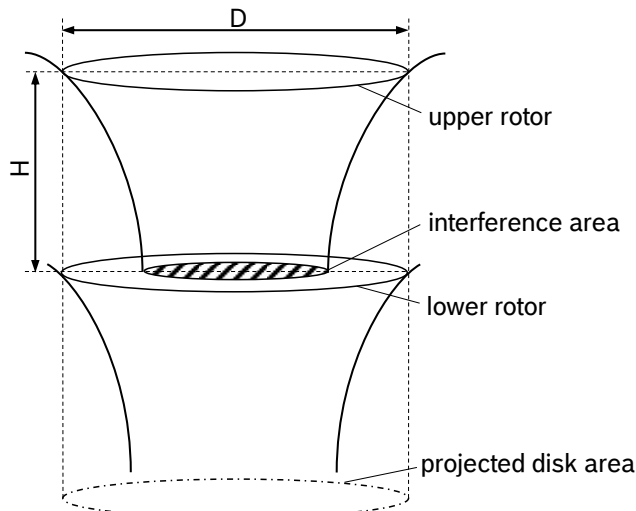


Figure 1: Contracting wake of upper and lower rotor (based on [3])

The modified flow field will affect performance and efficiency. An empirical model for the influence of one rotor on the other is developed by Johnson [4]. This model uses the assumption of equal thrust between the two rotors. The method is based on the momentum theory where the calculation of the induced power is mainly based on the disk area of the rotor system. As shown in Figure 1, the projected disk area of the coaxial rotor is only one half of the disk area of two isolated rotors. Therefore, the coaxial rotor has twice the disk loading compared to two single rotors:

$$(1) \quad A_{coax} = \frac{1}{2} \cdot A_{isolated}$$

Providing the same thrust, the actuator disk method provides 41 % increased rotor power for a coaxial rotor system as compared to two isolated working rotors with same rotor diameter:

$$(2) \quad P_{isolated} = \sqrt{\frac{T^3}{2 \cdot \rho \cdot A_{isolated}}}$$

$$(3) \quad P_{coax} = \sqrt{\frac{T^3}{2 \cdot \rho \cdot \frac{1}{2} A_{isolated}}} = \sqrt{2} \cdot P_{isolated}$$

This increase in required induced power is valid for

a lower rotor that is fully working in the slipstream of the upper rotor for an axial separation distance of less than 0.1 rotor diameter (D). The actuator disk method assumes that only the interference area of the lower rotor is affected by the wake and the power loss is decreased for a high separation distance as the wake contracts. It is postulated that for an operation of the second rotor in the far wake at the vena contracta, the induced power only increases by 28 % [4]. This actuator disk analysis compares the coaxial rotor system to two completely isolated rotors. The reduction in power loss derives from the outer region of the lower rotor that is not affected by the wake of the upper rotor. Taking into account the projected disk area, the actuator disk method leads to an improved performance of the coaxial rotor compared to the single rotor. The exact behaviour of the influence of one rotor on another was subject on several theoretical and experimental investigations. Coleman [5] did a comprehensive analysis of literature on coaxial rotors.

Studies on coaxial rotors for helicopter rotors with variable pitch have been made in the early 50s for example by Cheeseman [6]. The influence of one rotor on another has been theoretically studied. Coleman [5] concludes in his analysis that, compared to a single-rotor with similar solidity, the coaxial rotor has been modelled to require 5 % less power in hover at the same projected disk area.

Ramasamy [7] and McAlister [8] conducted experimental studies on the hover performance of a coaxial rotor system with the boundary condition of torque balance between the two rotor systems and equal solidity. It is postulated that measuring the thrust of the upper and lower rotor is important because the aerodynamic environment of the upper and lower rotor is different at all axial separation distances. It is stated that the separation distance in hover alters the thrust sharing ratios between the two rotors. The efficiency of a rotor in hover can be described by the Figure of Merit (FOM). It is concluded that nearly 9 % improvement of the FOM of a coaxial rotor system compared to a single rotor with equal solidity can be achieved. It is also remarked that the upper rotor influences the lower rotor even when the separation distance is large [7]. A theoretical study by Nagashima [9] states that the separation distance is a cue factor for optimal performance of the rotor system. Other studies [10] conclude that a coaxial rotor has an approximately 10 % higher FOM at hover compared to a single rotor.

In contrast to the investigations mentioned above [4, 7, 8], the present study considers a rotor system without torque balance, as it can be used for multi-rotor aircraft. Contrary to other studies [11], the

upper and lower rotors are analysed separately and principal effects are derived from basic investigations for this new boundary condition.

3. EXPERIMENTAL SETUP

3.1. Current Study & analyzed flight conditions

By considering a multi-rotor VTOL aircraft, the different flight conditions have to be investigated. The first case that plays an important role when it comes to propulsion dimensioning is the hover case where the lift is fully generated by the rotors. The same rotor system is also tested at incident flow conditions.

Due to the use of electrical motors without mechanical coupling, the axial rotor separation can be changed in a wide range. Each of the rotors might be powered by a distinct motor, the separation distance between the two rotors can be freely chosen. As the current study focuses on multi-rotor systems, the individual coaxial rotor system no longer has to be operated in a torque balanced mode. The investigated rotor distances in the experimental study presented in this paper are between $0.08 D$ and $0.75 D$. These are adequate distances for the implementation of an electrical motor that is directly coupled to the rotor. The coaxial systems are compared to a single rotor system of half solidity at similar Reynolds conditions.

3.2. Investigated Rotor system & powertrain

The investigated rotor system shown in Figure 2, consists of two identical propulsion units and rotors for the upper and lower sections. The upper and lower rotors are counter-rotating and are set-up to produce thrust in the same direction. The rotors have foldable blades with a diameter of 15" and a fixed pitch of 5.2" according to the manufacturers' specifications. The blades are directly mounted to the rotor of the electric motor. The upper and lower rotor blades have identical geometries and profiles.

The analyzed rotor system is based on a propulsion system of the type *DJI 4114* with a rated maximum power of 500 W. The motor is designed for an Octocopter with a maximum takeoff mass of 6 kg to 11 kg. Therefore, the intended thrust of one motor is between 7.4 N and 15.9 N. The motor is controlled by a *Herkules 5* BLDC inverter (*HERS/ Electronic Development GmbH & Co. KG*) with integrated closed loop control. The test bench can be operated in a duty cycle mode, a current control mode and, a rotational speed control mode. The measurements conducted in this study focus on rotational speed equality between the two coaxial

rotors. Therefore, the rotational speed control mode was used.

3.3. Mechanical design

For an experimental investigation of the described multi-rotor system a versatile test bench was designed. The test bench allows continuous adjustment of the vertical separation distance up to $0.75 D$. The test bench that is shown in Figure 2 is developed for the measurement of scaled electrical drives with rotors of 10" to 18" diameter.

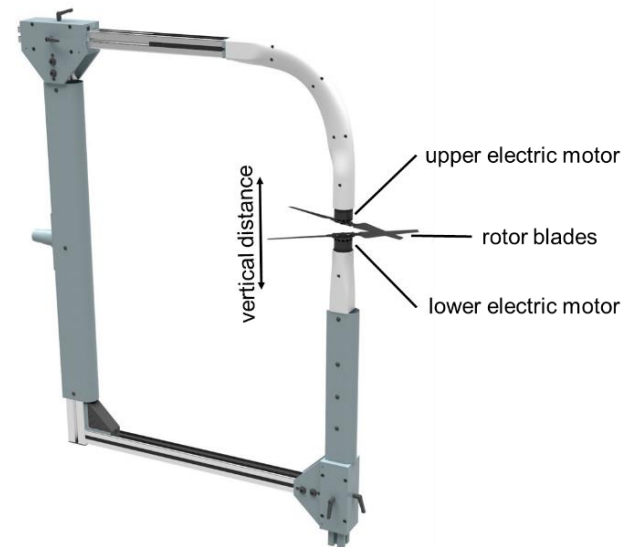


Figure 2: Mechanical design of the coaxial rotor test bench

The upper electric motor is directly coupled with the torque and force sensors, as illustrated in Figure 3, to avoid mechanical performance losses between rotor and sensor. The upper arm of the test bench is fabricated by a 3D printing method with an aerodynamically shaped profile to reduce wake effects of the structure on the rotors. Sensor and power cables are installed in separate tubes inside the test bench. To reduce aeromechanical effects in the wind tunnel, aerodynamic fairing panels were used to cover the arms of the test bench and to have a defined flow separation. The test bench can be used for hover tests with PIV (Particle Image Velocimetry) measurements in a measurement box at static thrust conditions or it can be mounted at a wind tunnel, e.g. at the subsonic wind tunnel of the "Institute of Aerospace Systems" (ILR) at RWTH Aachen. An adapter for the swivel mount is available.

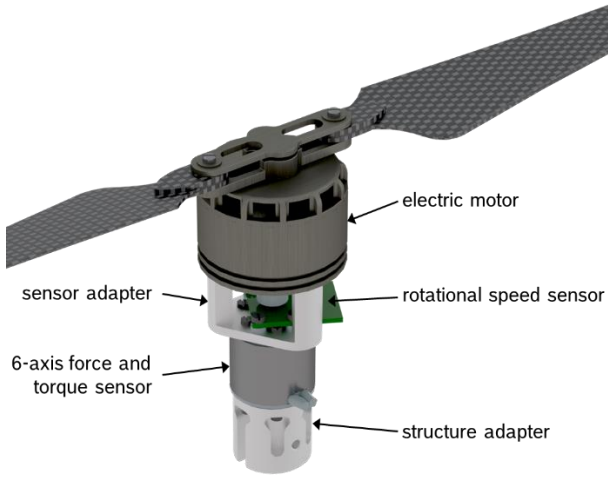


Figure 3: Propulsion unit with direct coupling of the force, torque and rotational speed sensor

For the analysis of different flight conditions, the angle of attack α can be adjusted by the swivel mount in the wind tunnel.

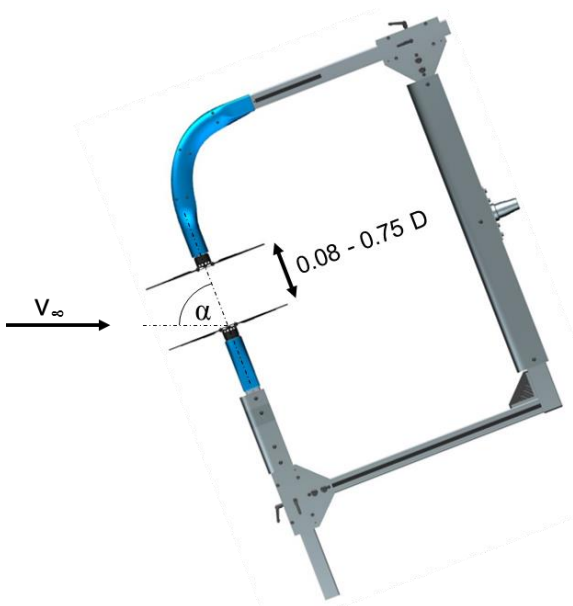


Figure 4: Analysed rotor system with different vertical separation distances at an angle of attack α

The rotor system in Figure 4 is tested in hover case with an angle of attack α of 90° . In cruise mode, the angle of attack is 0° . This is a propeller case where the rotor generates no lift. The wind tunnel experiments are performed for a range of the streamwise flow velocity v_∞ between 2 m/s and 16 m/s until the rotor reaches the windmill state. Windmill state is reached, when the rotors generate no thrust anymore.

3.4. Sensors and measurement system

As both rotors have to be analyzed separately, a separate sensor setup is implemented for each drive system. The measurement setup is based on a Controller Area Network Bus (CAN) communication system. All data are simultaneously acquired by the measurement system *IMC-Studio*. Each propulsion system has the following measured variables with the maximum values and the accuracy mentioned in Table 1:

sensor	maximum values	Resolution / Accuracy	temperature drift	
AS5147P	28000 rpm	4096 steps/revolution	-	
LAH 100-P	I_{\max} 100 A	$\pm 0.25\%$	max 0.5 mA	
K6D27	F_{z1} : 50 N	± 0.1 N	$\pm 0.05\%$ AV/K	$\pm 0.1\%$ FS/K
	M_{z1} : 1 Nm	± 0.005 Nm	$\pm 0.05\%$ AV/K	$\pm 0.1\%$ FS/K
	F_{z2} : 50 N	± 0.25 N	$\pm 0.05\%$ AV/K	$\pm 0.1\%$ FS/K
	M_{z2} : 1 Nm	± 0.004 Nm	$\pm 0.05\%$ AV/K	$\pm 0.1\%$ FS/K

Table 1: Maximum values and accuracy of the sensors (AV = actual value; FS = fullscale)

- Force and torque are measured in all 6 degrees of freedom by the *K6D27* sensor, manufactured by *ME-Messsysteme*. The sensor is directly mounted below the electrical motor to ensure accurate measurements. The force and torque range of the sensor is calibrated for the maximal expected forces in the z-component of 50 N.
- Input current and voltage to the BLDC inverter is measured by a *LAH 100-P* hall effect based current transducer from *LEM International SA* and by a voltage measurement module.
- The rotational speed is measured by interfacing an *AMS AS5147-TS_EK_AB* high speed rotational sensor to an Arduino which provides in addition the current rotor angle. The rotor angle is especially important when it comes to phase locked PIV measurements that are planned for further studies. The sensor sends its data via Serial Peripheral Interface to an Arduino and the processed data is sent via CAN to the *IMC Studio* system.
- The temperature is measured at the inverter and at the nozzle of the wind tunnel.

3.5. PIV equipment

The PIV equipment consists of a *pco. Sensicam qe* with a resolution of 1376 x 1040 pixels with a 50 mm lens with an aperture of 1:1.8. A double pulsed quantel Twins laser with a maximum energy of 400 mJ per pulse shapes a laser sheet in the plane of the symmetry axis of the rotor. The glycol and water based seeding is generated by a *Martin JEM ZR25* fog generator. All data is acquired by the commercial software *LaVision DaVis*.

4. EXPERIMENTAL INVESTIGATION AND RESULTS

In this chapter the results of the experimental investigation in hover and at an angle of attack $\alpha = 0^\circ$ with various flow velocities will be presented.

4.1. Analysis of isolated upper and lower rotors

For an evaluation of the coaxial system the behavior of the upper and lower rotor will be analyzed. Both rotors are observed separately as a first step. The rotors are analyzed for static thrust at rotational speeds between 1500 rpm and 6500 rpm. The non-active rotor is completely outside the flow field.

In Figure 5 the thrust of the isolated upper and lower rotor is visualized over the rotational speed. The thrusts generated by the two rotors are almost identical up to a rotational speed of 6200 rpm.

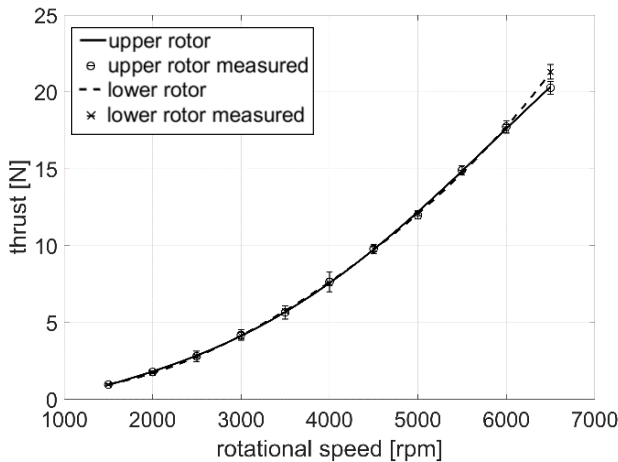


Figure 5: Thrust over rotational speed for the isolated upper and lower rotor

The corresponding required power is also measured and plotted in Figure 6. The same behavior as in Figure 5 can be observed. The power curve has also an approximately identical behavior for both rotors up to 6200 rpm.

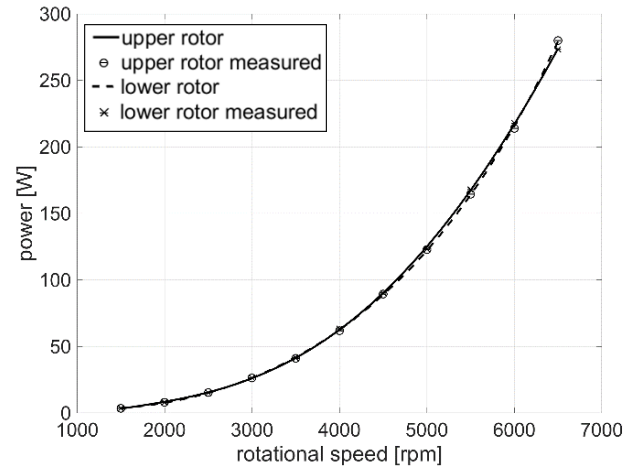


Figure 6: Required power over rotational speed for the isolated upper and lower rotor

Since the power curves as well as the thrust curves of the isolated rotors correspond well up to 6200 rpm, the rotors can be regarded as identical up to this rotational speed. Slight differences in thrust at highest rotational speeds of 6500 rpm can be explained by an interference with the support structure that becomes relevant at high flow speeds.

For a comparison of the single rotor to the coaxial rotor system, a coefficient to describe the efficiency is needed. The Figure of Merit is an important performance indicator for a hovering rotor. It is defined as the ratio between ideal and real power required for hover:

$$(4) \quad FOM = \frac{P_{ideal}}{P_{real}}$$

The ideal power for a rotor in hover for a measured thrust $T_{measured}$ is mainly dependent on the rotor disk area A :

$$(5) \quad P_{ideal} = \sqrt{\frac{T_{measured}^3}{2 \cdot \rho \cdot A}}$$

The real needed power is calculated by a multiplication of the measured torque M at the rotor shaft and the rotational speed of the rotor n :

$$(6) \quad P_{real} = 2 \cdot \pi \cdot M \cdot n$$

The Figure of Merit is calculated for different rotational speeds and plotted in Figure 7. With higher rotational speeds the FOM increases and reaches a maximum at the highest measured rotational speeds. Here the FOM is approximately slightly higher than 0.465. A full scale helicopter rotor has a FOM in the range of 0.6 to 0.7 [12].

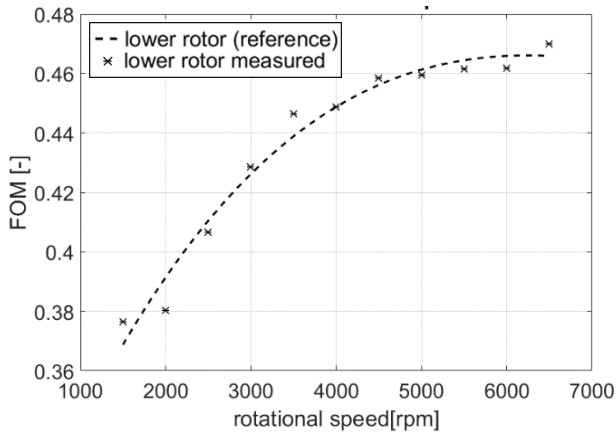


Figure 7: FOM over rotational speed for the isolated lower rotor (reference rotor)

4.2. Analysis of the coaxial rotor system in hover condition

In this chapter the measurements of the coaxial rotor system for several separation distances at hover are presented. The static thrusts of the upper and lower coaxial rotors are measured for various separation distances.

Figure 8 shows the thrust curves of the upper and lower rotor for separation distances H/D of 0.08, 0.2 and 0.5. The upper rotor produces more thrust for all separation distances than the lower rotor. However, for the smallest separation distance of 0.08, the thrust of both rotors is nearly identical. The average thrust of the two rotors stays approximately constant, independent of the configuration. This correlates quite well with the conclusion by Coleman [5] for torque balanced coaxial rotors that show a similar behavior. As it can be seen in Figure 8, the difference between the thrust of the two rotors decreases with decreasing separation distance.

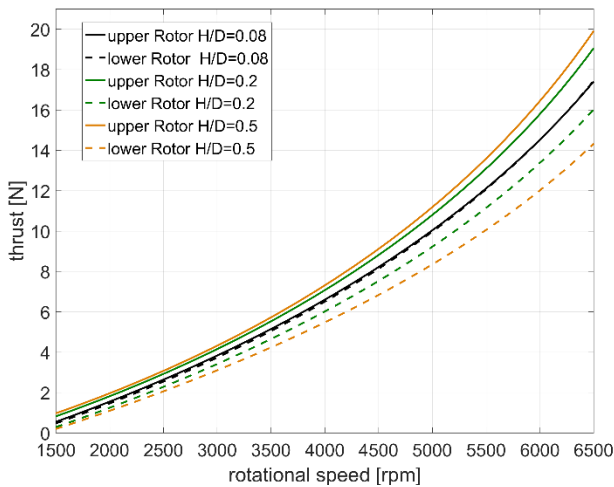


Figure 8: Thrust over rpm for different vertical separation distances

Besides the thrust sharing, the FOMs of the upper and lower rotor, as well as the combined FOM is important to evaluate the rotor system. Calculation of the FOM using formula (4) shows that the FOM of the upper rotor is higher than the FOM of the lower rotor due to the fact that it is influenced by the wake of the upper rotor to a significant part, as shown in Figure 1. From Figure 9, the FOMs of the upper and lower rotor are close to each other for small separation distances. Increasing the separation distance increases the difference in FOM between upper and lower rotor. The FOM of the lower rotor rapidly decreases and the FOM of the upper rotor increases at the same time.

An important factor for coaxial rotor systems is the combined FOM [13]. This metric is especially important when it comes to efficiency comparison of different rotor systems with equal boundary conditions. The following definition of the FOM is used in this study to compare the different separation distances:

$$(7) \quad FOM_{comb} = \frac{\sqrt{\frac{(T_{upp} + T_{low})^3}{2 \cdot \rho \cdot A}}}{(2 \cdot \pi \cdot M_{upp} \cdot n_{upp}) + (2 \cdot \pi \cdot M_{low} \cdot n_{low})}$$

In Figure 9 the combined FOM is shown for a varying rotor separation distance. The combined FOM deteriorates only slightly with increased rotor separation distance. Compared to the single rotor where the FOM at 5000 rpm is approximately 0.465, the combined FOM of the coaxial rotor system in a rotational speed equality mode is slightly higher. It reaches a maximum FOM of 0.488 at a separation distance H/D of about 0.13.

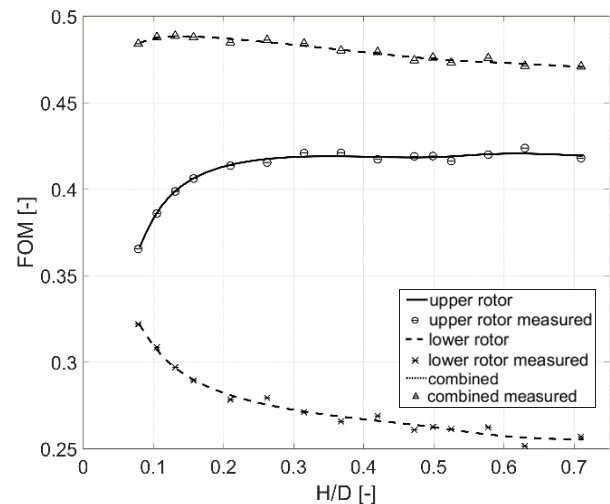


Figure 9: FOM over rotor separation distance for the upper and lower rotor at 5000 rpm

4.3. Analysis of the coaxial rotor system in an axial incidence flow condition ($\alpha = 0^\circ$)

In addition to the static thrust measurements, the rotor system is measured at an angle of attack α of 0° for incident flow conditions up to the windmill state where the rotors no longer produce thrust. Until this state is reached, the upper rotor produces additional thrust by a factor of over 1.6.

As the definition of the Figure of Merit can only be used in hover, the quality of the rotor system at $\alpha = 0^\circ$ is described by the efficiency η . It can be calculated by the following formula [14]:

$$(8) \quad \eta = J \cdot \frac{C_T}{C_P}$$

With the advance ratio J :

$$(9) \quad J = \frac{v}{n \cdot D}$$

and thrust and power coefficients:

$$(10) \quad C_T = \frac{T}{\rho \cdot n^2 \cdot D^4}$$

$$(11) \quad C_P = \frac{P}{\rho \cdot n^2 \cdot D^5}$$

The coaxial rotor is analyzed for a separation distance H/D of 0.08 and 0.5. As it can be seen in Figure 10, the upper rotor is operating at a significantly higher efficiency than the lower rotor for both separation distances. It is remarkable that the efficiency of the upper rotor is nearly independent of the separation distance at $\alpha = 0^\circ$ and it is approximately equal to the isolated rotors efficiency. The efficiency of the upper rotor changes only slightly in contrast to the hover case where the FOM of the upper rotor strongly depends on the separation distance. The main reason for the independence of the efficiency of the upper rotor from the separation distance is the predominance of the incidence flow and only a small upstream effect of the lower rotor on the upper rotor.

However, the efficiency of the lower rotor becomes higher with decreasing rotor separation distance as shown in Figure 10. The effect on efficiency on the lower rotor for different separation distances is in good agreement with the results of the hover case that is described in chapter 4.2.

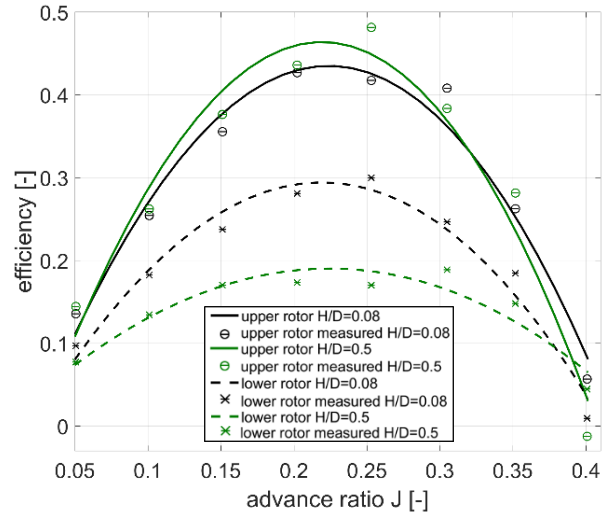


Figure 10: Efficiency comparison of the upper and lower rotor in axial incidence flow conditions compared at $H/D=0.08$ and $H/D=0.5$ at $\alpha = 0^\circ$ for various advance ratios J

4.4. Flow field analysis with Particle Image Velocimetry (PIV)

To evaluate the performance characteristics determined by the previous force measurements, the flow field is analyzed with the PIV method. Force measurements clearly show that the lower rotor works in an operation point with lower Figure of Merit. The flow field of a coaxial rotor system with a separation distance H/D of 0.2 is measured at a rotational speed of 5000 rpm.

A final interrogation windows size of 32×32 pixels with 75 % overlap leads to a resolution of approximately 0.5 vectors/mm. Only every fourth vector is shown in the images below. The PIV measurements are averaged over 250 images. Figure 11 shows the averaged vorticity distribution over several phase angles.

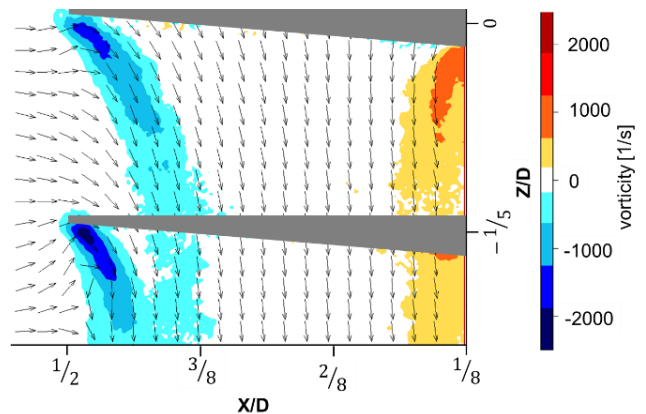


Figure 11: Vorticity field of the coaxial rotor system with $H/D=0.2$ H/D at 5000 rpm

The vortices at the tip of the blades contract to the inside of the lower blade and hit the lower rotor at approximately 0.8 D. The arrows in Figure 11 show the direction of the flow. A strong cross-flow component can be observed at the tip of the lower blade.

The velocity of the vertical flow direction is visualized in Figure 12. The velocity between the two rotors is in the range of 10 to 12 m/s directly under the upper rotor and accelerates up to 14 m/s until it reaches the plane of the lower rotor although the inflow velocity at the tip of the lower blades is still significantly lower. This results in a strong velocity gradient between the outer and inner region of the blade. The inhomogeneous and high inflow velocity at the lower rotor leads to a lower FOM of this rotor.

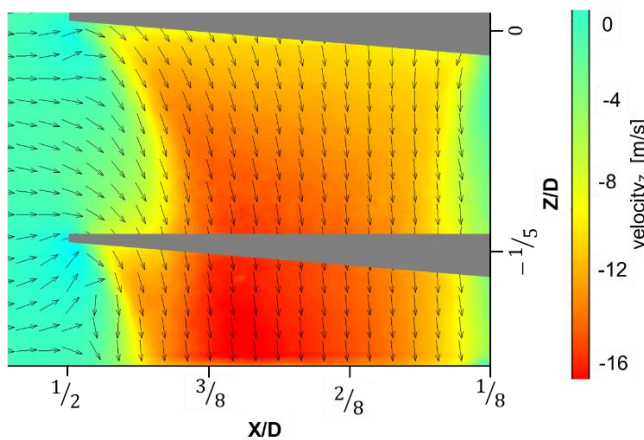


Figure 12: Velocity field of the coaxial rotor system with $H/D=0.2$ at 5000 rpm

5. CONCLUSION

The presented study focuses on a coaxial rotor system with equal rotational speeds of the upper and lower rotor. Performance of the upper and lower rotors have been analyzed separately by a coaxial rotor test bench and the flow field was analyzed by PIV.

In the hover case, the combined FOM of the coaxial rotor system is nearly independent from the vertical rotor separation distance. By regarding the performance of the upper and lower rotor individually, it can be observed that it highly depends on the rotor distance. A higher rotor distance results in an improved FOM of the upper rotor and in a decrease of the FOM of the lower rotor. For very small separation distances, the FOMs of the upper and lower rotor are close to each other.

A flow field visualization shows the flow between the two rotors. A strong gradient between the velocities from the inner interference area to the

outer region of the lower rotor is visible and a strong crossflow component at the outer part of the lower blade is identified.

The same coaxial rotor system was tested at an angle of attack α of 0° . The overall efficiency highly depends on the rotor distance. In contrast to the hover case, the combined efficiency improves with lower rotor distance. The upper rotor performance remains almost constant regardless of the rotor distance. The increased performance of the lower rotor with smaller separation distance is consistent with the results in hover.

The findings of this study have an influence over the coaxial rotor system design. For the investigated rotor system with the boundary condition of rotational speed equality and rotor geometry equality it can be concluded that a rotor system with a separation distance as small as possible should be preferred. This is beneficial at an angle of attack α of 0° and has a slight influence in hover considering the overall rotor system performance. The power requirements for both rotors are of the same magnitude for small separation distances.

This investigation is focused on coaxial rotor configurations with special boundary conditions regarding rotational speed and geometry equality. Two optimization changes can be considered for further investigations. The first possibility is to investigate the effect of different rotational speed ratios between the two rotors, to achieve better inflow conditions at the lower rotor. A second possibility would be to adapt the pitch angle of the rotor blades in a further study.

References:

- [1] Balac, M.; Vetrella, A. R.; Axhausen K. W.: Towards the integration of aerial transportation in urban settings. In: Arbeitsberichte Verkehrs- und Raumplanung 1266, 2017.
- [2] Bondyra, A.; Gardecki, S.; Gąsior, P.; Giernacki, W.: Performance of coaxial propulsion in design of multi-rotor UAVs. In: Challenges in Automation, Robotics and Measurement Techniques. Springer, Cham, pp. 523-531, 2016.
- [3] Leishman, G. J.: Principles of helicopter aerodynamics with CD extra. Cambridge: Cambridge University Press, ISBN 0-521-85860-7, 2006.
- [4] Johnson, W.: Helicopter theory. New York: Courier Corporation, ISBN 978-0-486-68230-3, 1980.

- [5] Coleman, C. P.: A survey of theoretical and experimental coaxial rotor aerodynamic research. In: NASA TP-3675, 1997.
- [6] Cheeseman, I. C.: A method of calculating the effect of one helicopter rotor upon another. In: A.R.C. Technical Reports C.P. No. 406, 1958.
- [7] Ramasamy, M.: Measurements comparing hover performance of single, coaxial, tandem, and tilt-rotor configurations. In: American Helicopter Society 69th Annual Forum. Vol. 31, 2013.
- [8] McAlister, K. W.; Tung, C.; Rand, O.; Khromov, V.; Wilson, J.S.: Experimental and numerical study of a model coaxial rotor. In: American Helicopter Society 62nd Annual Forum, Phoenix, AZ, 2006.
- [9] Nagashima, T.; Nakanishi, K.: Optimum Performance and Wake Geometry of Co-Axial Rotor in Hover. In 7th European Rotorcraft Conference Garmisch-Partenkirchen, 1981.
- [10] Bourtsev, B. N.; Kvokov, V. N.; Vainstein, I. M.; Petrosian, E. A.: Phenomenon of a coaxial helicopter high figure of merit at hover. In: 23rd European Rotorcraft Conference Dresden, 1997.
- [11] Harrington, R. D.: Full-Scale-Tunnel Investigation of the Static-Thrust Performance of a Coaxial Helicopter Rotor. In NACA TN 2318, 1951
- [12] Van der Wall, B. G.: Grundlagen der Hubschrauber-Aerodynamik, Berlin Heidelberg: Springer Vieweg, ISBN 978-3-662-44399-6, 2015.
- [13] Leishman, J. G.; Syal, M.: Figure of merit definition for coaxial rotors. In: Journal of the American Helicopter Society 53.3, pp. 290-300, 2008.
- [14] McLemore, H. C.; Cannon, M. D.: Aerodynamic Investigation of a four-blade propeller operating through an angle-of-attack range from 0 to 180 degrees. In: NACA TN 3228, 1954.